

Martin Baumann^{*1}, Vincent Heuveline¹, Leonhard Scheck², and Sarah C. Jones²¹Engineering Mathematics and Computing Lab (EMCL)²Institute for Meteorology and Climate Research (IMK)

Karlsruhe Institute of Technology (KIT), Germany

1. INTRODUCTION

The dynamics of tropical cyclones (TCs) can be influenced on a wide range of spatial and temporal scales. The numerical modeling of such multi-scale problems is challenging, since not all of the small-scale features can be well-resolved in large spatial domains due to limited computing capacities. Therefore, adaptive methods which allow for varying mesh resolution are promising, since relevant regions can be investigated in more detail by using higher mesh resolution locally. But due to the physical coupling of the processes in the atmosphere and the effect of advection, errors that have developed somewhere in the domain earlier in time, might grow and prolongate even to regions of high resolution at which the error was meant to be small. Hence, the fundamental question remains at which regions of the domain the local mesh resolution of the discrete model should be kept high to keep the error with respect to some user-defined measure small.

We consider a goal-oriented adaptivity approach based on the Dual Weighted Residual (DWR) method (Eriksson et al., 1995; Bangerth and Rannacher, 2003). The error measure is defined in terms of some output functional which represents a feature of the solution that should be determined very accurately. The influence of perturbations on this functional – denoted as goal-functional in that context – can be valued by means of adjoint sensitivity which is the solution of a corresponding dual problem. This sensitivity information represents a major ingredient for the overall adaptive method since it allows to estimate each cell's contribution to the error in the goal-functional. These contributions can be used to guide the mesh-adaptation process towards an efficient discretization.

We apply this generic approach of mesh adaptation to a scenario of binary tropical cyclone interaction and focus on the precise prediction of the storm track. We introduce a goal-functional that is strongly correlated with the storm position. Approximate solutions of this scenario corresponding sensitivity information are calculated based on a space-time finite element discretization. Adaptation of the spatial mesh by local mesh refinement and coarsening and the use of optimal time steps which both

are determined based on the estimated error contributions lead to significant gain in efficiency of the discrete model. The investigated physical model is simple (i.e. two-dimensional; barotropic; no effects of temperature and moist), but the applied concept of goal-oriented error estimation and adaptation are generic. Therefore, the presented results clearly show the great potential of such techniques to improve the efficiency of TC models.

2. MODEL AND DISCRETIZATION

2.1 Physical model

The dynamics of tropical cyclones can be described approximately using a non-divergent barotropic model. We neglect the contribution of the Earth's rotation and denote by $\Omega := [-L_1, L_1] \times [-L_2, L_2] \subseteq \mathbb{R}^2$ ($L_1, L_2 \in \mathbb{R}$) the spatial domain and by $[0, T]$ the time horizon. The vector-valued function $v : [0, T] \times \Omega \rightarrow \mathbb{R}^2$ denotes the velocity field and $p : [0, T] \times \Omega \rightarrow \mathbb{R}$ the scalar pressure field. For the kinematic viscosity $\nu > 0$ and initial velocity field v_0 , the time-dependent incompressible Navier-Stokes equations have the form:

$$\begin{cases} \partial_t v + (v \cdot \nabla)v - \nu \Delta v + \nabla p & = 0, & \text{in } [0, T] \times \Omega, \\ \nabla \cdot v & = 0, & \text{in } [0, T] \times \Omega, \\ v(0, x) & = v_0(x), \quad \forall x \in \Omega. \end{cases} \quad (1)$$

We imply space-periodic boundary conditions, such that the velocity and pressure fields must fulfill

$$v(t, x + L_i e_i) = v(t, x), \quad p(t, x + L_i e_i) = p(t, x), \quad (2)$$

for any $(t, x) \in [0, T] \times \Omega$ and $i \in \{1, 2\}$, where $e_1 := (1, 0)^T$, $e_2 := (0, 1)^T$. The techniques of goal-oriented error estimation and adaptation presented in Section 3 will be described based on a space-time finite element method for a corresponding variational formulation of problem (1)-(2), given in the following.

But before, some notations and function spaces are introduced. The space of trial functions for the velocity is denoted by X and contains continuous functions in time. Y denotes the space of test functions for the velocity and M the space of test and trial spaces for the pressure. Functions in Y and M don't need to be continuous in time. $(a, b) := \int_{\Omega} a(x) b(x) dx$ denotes the scalar product of two

^{*}Corresponding author address: Martin Baumann, Engineering Mathematics and Computing Lab (EMCL), Karlsruhe Institute of Technology (KIT), Fritz-Erler-Str. 23, 76133 Karlsruhe, Germany; e-mail: martin.bauman@kit.edu.

square-integrable functions a and b . Further details on these function spaces and concepts can be found e.g. in (Emmrich, 2004).

2.2 The primal problem

Now the variational formulation can be given. The functions $(v, p) \in X \times M$ denote a weak solution of problem (1)-(2), if it holds

$$\rho(v, p)(\varphi, \psi) = 0, \quad (3)$$

for all test functions $(\varphi, \psi) \in Y \times M$. Problem (3) is denoted the *primal problem* in the following. Here, the residual ρ is defined in terms of integrals in time and space by

$$\begin{aligned} \rho(v, p)(\varphi, \psi) := & \int_0^T \left((\partial_t v + (v \cdot \nabla)v, \varphi) + \nu(\nabla v, \nabla \varphi) \right. \\ & \left. - (p, \nabla \cdot \varphi) + (\nabla \cdot v, \psi) \right) dt \\ & + (v|_{t=0} - v_0, \varphi|_{t=0}). \end{aligned}$$

2.3 The dual problem

The *dual problem* allows to quantify the sensitivity that perturbations of the solution $v \in X$ of problem (3) have on some user-defined *goal-functional* $J : X \rightarrow \mathbb{R}$. This functional represents a quantity, that is of interest for the current investigation. The dual problem can be derived as described for optimization problems, see e.g. (Hinze et al., 2008). It is posed backward in time and has the following form: Find $(z, q) \in X \times M$ such that it holds

$$\rho^*(z, q)(\varphi, \psi) = 0 \quad (4)$$

for all test functions $(\varphi, \psi) \in Y \times M$. The dual residual ρ^* is defined by

$$\begin{aligned} \rho^*(z, q)(\varphi, \psi) := & \int_0^T \left(-(\partial_t z, \varphi)_\Omega + ((v \cdot \nabla)\varphi + (\varphi \cdot \nabla)v, z) \right. \\ & \left. + \nu(\nabla \varphi, \nabla z) - (\nabla \cdot z, \psi) + (\nabla \cdot \varphi, q) \right) dt \\ & + (z|_{t=0}, \varphi|_{t=0}) + \nabla J(v)\varphi. \end{aligned}$$

The goal-functionals used for the numerical runs in Section 4 will be defined as integral over the domain Ω at the final time T , i.e. $J(v) := (j(v|_{t=0}), z|_{t=0})$. In this case, the linearization $\nabla J(v)\varphi$ represents the initial condition of the dual problem which corresponds to the final time T . Further details can be found in (Baumann, 2011).

2.4 Space-time finite element discretization

We applied a conforming space-time finite element method based on a partitioning of the time interval $[0, T]$, $0 = t_0 < \dots < t_{N_{\text{time}}} = T$, and a triangulation of the domain Ω into N^{space} quadrilaterals. For the discretization, the function spaces $X_h \subset X$, $Y_h \subset Y$ and $M_h \subset M$ are defined as described in the following. In each interval (t_{i-1}, t_i) ,

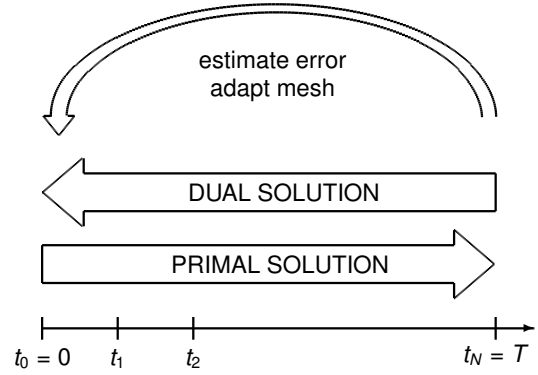


FIG. 1: Iterative procedure of calculation of primal and dual solution, error estimation and adaptation.

the velocity function is linear in time and globally continuous. All test functions as well as the pressure function are piece-wise constant in time, with jumps at t_i ($i = 1, \dots, N$). This time-discretization leads to a time-stepping scheme, since the discontinuous test functions decouple the global problem. This approach is based on the cGP(1)-method described in (Schieweck, 2010). For the discretization in space, stable Taylor-Hood elements are applied, see e.g. (Ern and Guermond, 2004). On each quadrilateral, the velocity function is bi-quadratic and the pressure bilinear, and both are globally continuous. For the primal and the dual problems (3) and (4) these discrete function spaces lead to finite-dimensional systems.

3. ERROR ESTIMATION AND MESH ADAPTATION

In this section, we describe an adaptivity approach of the space and time discretization that leads to more efficient methods for the determination of the quantity of special interest for the investigator. The spatial mesh is refined or coarsened and the time step sizes are chosen based on *error indicators* that are part of an *a posteriori error estimator* described in the following.

Let $v_h \in X_h$ be the velocity field of the discrete solution of the primal problem (3). For the goal-functional J , the solutions defect with respect to the quantity of interest is $J(v) - J(v_h)$, where $v \in X$ denotes the exact velocity field of the primal problem. For this error quantity, an evaluable error characterization can be given by an a posteriori error estimator (Bangerth and Rannacher, 2003; Baumann, 2011), known in the context of the Dual-Weighted Residual (DWR) method:

$$\begin{aligned} |J(v) - J(v_h)| & \approx E(v_h, p_h, z_h, q_h) \\ & \leq \sum_{i=1}^{N^{\text{space}}} \eta_i^{\text{space}} + \sum_{j=1}^{N^{\text{time}}} \eta_j^{\text{time}}. \end{aligned}$$

The estimator E is defined in terms of the primal residual ρ and the dual residual ρ^* and makes use of patch-wise higher-order interpolation as described in (Bangerth and

Rannacher, 2003). The spatial error indicator η_i^{space} represents the maximal contribution of cell i to the error in J over the complete time interval $[0, T]$. Analogously, the temporal error indicator η_j^{time} represents the maximal error contribution of time interval (t_{j-1}, t_j) taken over all quadrilaterals in the triangulation. Based on these error indicators, the triangulation of the domain and the partitioning of the time interval can be adapted, such that the space-time mesh consists of a user-defined number of cells and time steps.

The overall adaptive method is an iteration, and each loop has three phases. First, the primal and dual solutions are calculated based on a given mesh and time partitioning. Then, the error indicators with respect to the spatial and temporal time discretization can be determined. Finally, the spatial mesh and the time steps can be adapted correspondingly, see Fig. 1.

The adaptive numerical simulations presented in the following includes techniques of local mesh refinement or coarsening (h-adaptivity) and optimal time step size determination. Cells with large error indication are refined into four smaller cells and cells with very small contribution are marked to be coarsened. Four neighboring cells are coarsened to one bigger cell only if each of the four cells was marked to be coarsened. This procedure leads to so-called *hanging nodes* which are treated conformingly, i.e. global continuity is guaranteed. We also investigated an approach of mesh deformation (r-adaptivity), where mesh points are moved to regions of the domain, at which high resolution is needed. Although the number of cells remains constant, the resulting error in the goal-functional can be strongly decreased by such mesh optimization techniques, see (Bauer et al., submitted). The optimal time step size can be chosen such that the temporal error indicators are approximately equally distributed over the partitioning of the time interval.

4. NUMERICAL RESULTS

4.1 Scenario: Binary tropical cyclone interaction

The interaction of two TCs is investigated based on a barotropic model. The storms are represented by two vortices that are closely located at initial time such that their profiles overlap. During the first hours, the storms start orbiting around each other. Depending on the initial separation distance, the TCs can either merge or diverge from one another.

The considered domain has doubly periodic boundary conditions, i.e. $\Omega := [-L_1, L_1] \times [-L_2, L_2]$, where $L_1 = 2000$ km and $L_2 = 1732$ km. The initial separation of the storms is $D = 400$ km and the initial positions are $(-D/2, 0)$ and $(D/2, 0)$. The symmetrical storm profiles are defined in terms of their tangential wind field v_T as introduced in (Smith et al., 1990):

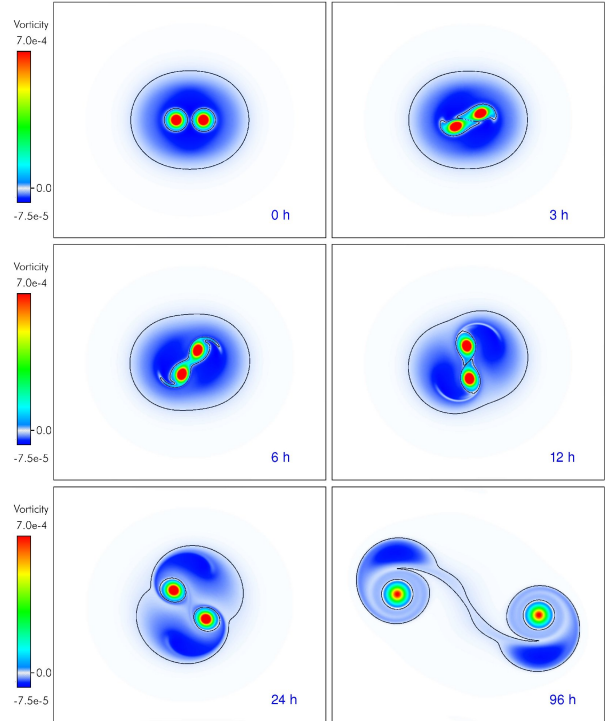


FIG. 2: Development of two idealized tropical cyclones.

$$v_T(s) := \tilde{v} \frac{s(1 + (6b/2a)s^4)}{(1 + as^2 + bs^6)^2}, \quad s := r/r_0,$$

with $a = 0.3398$, $b = 5.377 \times 10^{-4}$, $\tilde{v} = 71.521$ m/s and $r_0 = 100$ km. For these parameters, the maximal tangential wind is 40 m/s at the radius $r = r_0$. The initial condition of the velocity field v_0 is the sum of the two velocity profiles for the two storms. The dynamical evolution is investigated for a time horizon of $T := 96$ h.

In Fig. 2, the motion and development of the two storms is visualized in terms of the vorticity, i.e. the curl of the velocity field. Red areas indicate high vorticity regions and represent the storm centers. Dark blue regions indicate zones of negative vorticity represent the anticyclonic outflow of real TCs. During the first hours, the two vortices start orbiting around each other. In this phase, the cores are strongly deformed and temporarily connected. The zone of negative vorticity around the cores is restructured and after 12 hours, two separate negative vorticity regions have developed which can be interpreted as anticyclones. Together with the positive cores they form two cyclone-anticyclone pairs that start to propagate away from each other along straight tracks.

The moment at which the motion turns from orbiting into straight direction determines the final direction of the storm tracks. Small perturbations in the initial state can influence when this transition takes place and thus can have a strong influence on the final storm positions. The high sensitivity to the initial conditions is also evident from

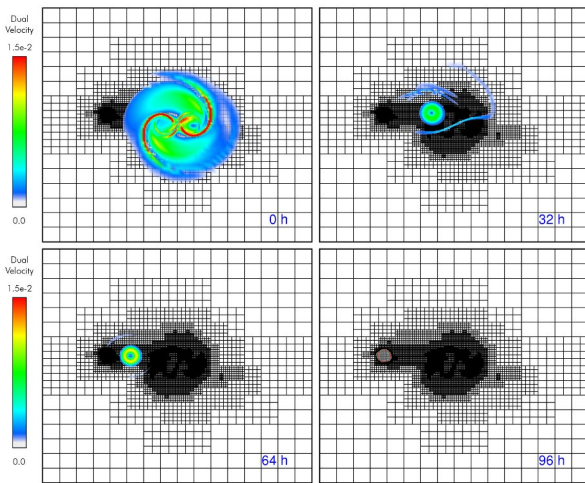


FIG. 3: Dual velocity (i.e. sensitivity information) and optimized mesh with approximately 120,000 DOFs.

the fact that for a slightly smaller initial separation, a qualitatively different solution is found – the two TCs merge. For these reasons, this scenario has been chosen as a benchmark problem for adaptive methods.

4.2 Adaptive simulations

We carried out adaptive numerical simulations of the binary cyclone interaction scenario. In the following investigation, we chose the storm that has final position on the upper left side after 96 hours as the one that should be approximated very accurately and represents the quantity of interest. The storm position is characterized by the region of maximal vorticity. We introduced a goal-functional which is strongly correlated to the storm position. It is defined as vorticity, integrated over that storm's core after 96 hours of development. The region that defines the core is approximated by a circle around the storm center $P = (-1043.678 \text{ km}, 153.365 \text{ km})$ with radius of $R = 93 \text{ km}$:

$$J(v) := \int_{B(P,R)} \nabla \times v(x, T) dx.$$

At the radius R , the vorticity is approximately 50% lower than at the center and the vorticity gradient is strong. Therefore, small changes of the storm position have strong influence on the vorticity integral given by J . For this goal-functional, the reference value is $J(v) = 14.486 \text{ km}^2/\text{s}$. The two parameters P and R were determined from high-resolution reference simulations. Although such parameters are not known a priori in general, they can be determined from approximate solutions that have been calculated already when the dual problem has to be solved, see Section 3.

Since the two storms are in interaction during the initial phase, the second storm has also great influence on the

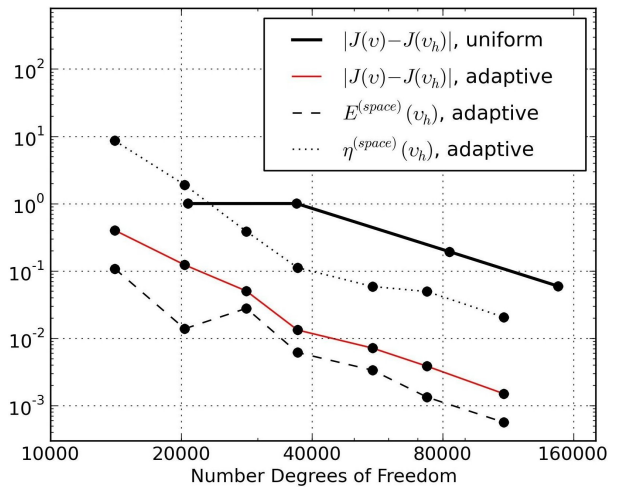


FIG. 4: Relative error in goal-functional J for several uniform and locally refined meshes.

final position of the first one. One question to be addressed is to what extent this influence will be accounted for by the adaptive method and the resulting optimized meshes.

For this goal-functional, we calculated error indicators and adapted the mesh and time steps as described in Section 3 using the multi-purpose finite element library HiFlow³ (Heuveline, 2010). Since the exact solution is not known for this scenario, a reference solution based on a spatial mesh with 1,327,104 degrees of freedom (DOFs) with a cell diameter of approximately 10 km and 1,152 time steps was calculated. For the error analysis, the resulting reference solution v and corresponding storm position at final time is employed to quantify the different errors.

Fig. 3 shows the dual solution, i.e. the sensitivity information, corresponding to the goal-functional J calculated on an optimized mesh with about 120,000 DOFs. At initial time, the sensitive regions are almost symmetrically distributed and surround the regions of the initial positions of the two vortices. At this stage, the vortices are closely located and the subsequent storm tracks are significantly impacted by their mutual interaction. Although only one of the two storms is directly accounted for by the definition of the goal-functional, the sensitivity of both storms is high. It can be seen that the optimized mesh has high resolution at the region where both storms are located at these first hours of simulation. After 32 hours, the tendency of the sensitive regions to the storm on the left can clearly be seen. After 96 hours, these congregate at the outside radius of the circle where vorticity is approx. 50% of the maximal value. The track of the second storm is highly resolved as long as its influence on the track of the first storm is strong.

In Fig. 4, the relative error in the goal-functional $|J(v) - J(v_h)|/J(v)$ and corresponding estimated error

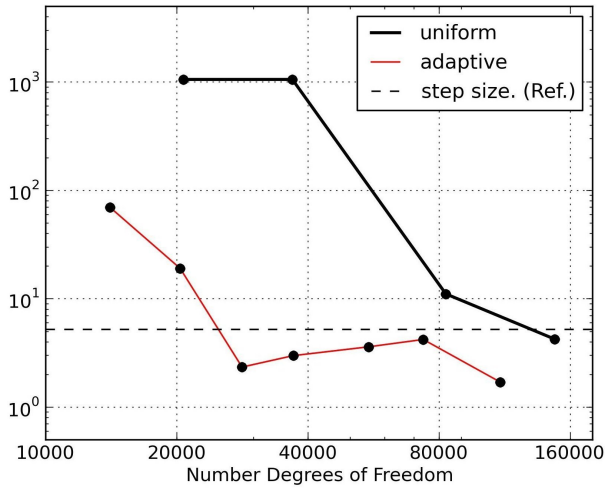


FIG. 5: Position error in km of the storm after 96 hours for several uniform and locally refined meshes.

quantities based on uniform and adapted meshes are plotted. The estimated and true error in the goal-functional show good agreement, especially on meshes with more than 30,000 DOFs. The resulting errors on optimized meshes, are reduced by more than one order of magnitude compared to uniform meshes (with approximately the same number of unknowns).

The position error after 96 hours is shown in Fig. 5. Even on grids with less than 20,000 DOFs, the tracks can be predicted qualitatively correct (i.e. the storms diverge) with a final position error below 100 km. The first mesh with final position error of less than 10 km has about 30,000 DOFs.

The optimization of the time-discretization based on the temporal error indicators η_j^{time} is investigated in the following, based on a locally refined mesh with 36,864 DOFs. Fig. 6 shows in black the temporal error indicators cor-

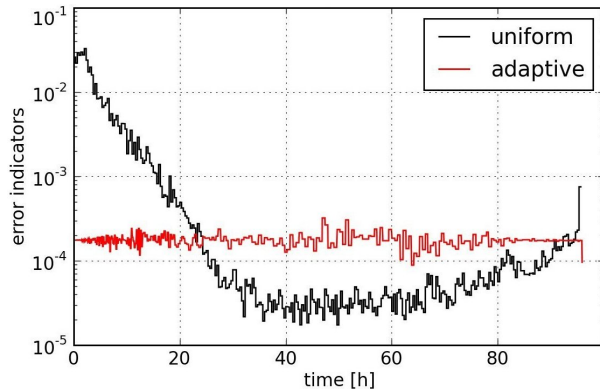


FIG. 6: Temporal error indicators η_j^{time} for an approximate solution, calculated on a time discretization with 288 intervals, plotted over the time.

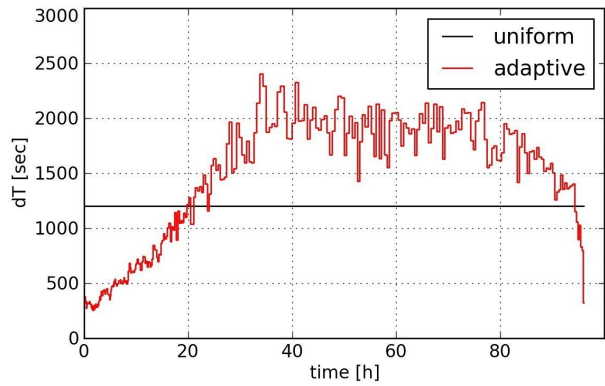


FIG. 7: Time increments of a time discretization with 288 intervals, plotted over the time.

responding to a uniform partitioning of the time interval. During the initial phase of mutual interaction of the storms, the error indication is significantly higher, compared to later times. By the iterative optimization procedure, described in Section 3, the time increments were adapted such that in this initial phase small time step sizes were applied, see red plot in Fig. 7. This lead to approximately equally distributed temporal error indicators within the total time interval, see red plot in Fig. 6.

For the investigated scenario, the optimization of the time step sizes leads to significant improvements. On adapted partitions, the position error was reduced by approximately one order of magnitude compared to uniform partitions with the same number of sub-intervals, see Fig. 8. For example, a prediction accuracy based on 576 uniform time-intervals could be obtained approximately on an optimized partitioning with only 144 increments. It must be noted that the adaptation of the time discretization can be accomplished independent of spatial mesh adaptation techniques and can improve the resulting efficiency of the discrete model strongly, as shown for this scenario.

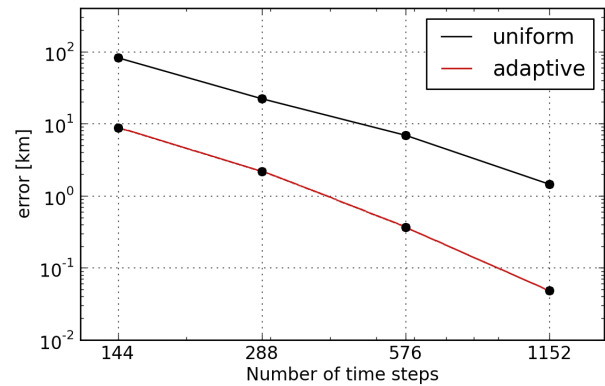


FIG. 8: Position error in km of the storm after 96 hours for several uniform and locally refined time partitionings.

5. OUTLOOK AND DISCUSSION

We presented a concept of goal-oriented error estimation and adaptation and conducted numerical runs for a scenario of binary tropical cyclone interaction. The approach is very general and can in general be applied to models of arbitrary complexity. The calculation of the required sensitivity information with respect to the quantity of interest requires the solution of a linearized, adjoint model. Its formulation and solution can be non-trivial, especially if model switches for different regimes are included (e.g. for convection).

Although we applied a simple barotropic model, the great potential such techniques have could clearly be seen in the numerical results. Based on the error indicators, arbitrary mesh adaptation techniques can be applied that are offered by the simulation software (e.g. h- and r-adaptivity or nesting techniques). Furthermore, the mesh can be adapted dynamically (in the extreme case in every time step) or statically (i.e. one mesh for the complete time interval). The spatial mesh and the time partitioning can be adapted independently of one another.

Next steps will cover the investigation of more complex, three-dimensional models that also include moist processes. Techniques to reduce the over-all computational cost will be addressed. In this context, efficient methods for approximate calculation of the sensitivity information based on reduced models will be investigated.

Acknowledgements

This research was supported by the German Research Foundation (DFG) priority programme (SPP) 1276.

REFERENCES

Bangerth, W. and R. Rannacher, 2003: *Adaptive Finite Element Methods for Differential Equations*. Birkhäuser Verlag.

Bauer, W., M. Baumann, L. Scheck, A. Gassmann, V. Heuveline, and S. Jones: Simulation of tropical-cyclone-like vortices in shallow-water icon-hex using goal-oriented r-adaptivity. *Manuscript submitted for publication*.

Baumann, M., 2011: *Numerical Simulation of Tropical Cyclones using Goal-Oriented Adaptivity*. PhD thesis, Karlsruhe Institute of Technology (KIT), Engineering Mathematics and Computing Lab (EMCL).

Emmrich, E., 2004: *Gewöhnliche und Operator-Differentialgleichungen: Eine integrierte Einführung in Randwertprobleme und Evolutionsgleichungen für Studierende*. Vieweg, Wiesbaden, 1. Aufl. edition.

Eriksson, K., D. Estep, P. Hansbo, and C. Johnson, 1995: Introduction to Adaptive Methods for Differential Equations. *Acta Numerica*, **4**(-1), 105–158.

Ern, A. and J.-L. Guermond, 2004: *Theory and practice of finite elements*. Applied mathematical sciences; 159. Springer, New York.

Heuveline, V., 2010: Hiflow3: a flexible and hardware-aware parallel finite element package. In *Proceedings of the 9th Workshop on Parallel/High-Performance Object-Oriented Scientific Computing*, POOSC '10, ACM, New York, NY, USA, 4:1–4:6.

Hinze, M., R. Pinnau, M. Ulbrich, and S. Ulbrich, 2008: *Optimization with PDE Constraints*. Springer.

Schieweck, F., 2010: A-stable discontinuous galerkin-petrov time discretization of higher order. *Journal of Numerical Mathematics*, **18**(1), 25–57.

Smith, R. K., W. Ulrich, and G. Dietachmayer, 1990: A numerical study of tropical cyclone motion using a barotropic model. I: The role of vortex asymmetries. *Quart. J. Roy. Meteor. Soc.*, **116**(492), 337–362.